

H. MEHRABAN, A. ASADI

Physics Department, Semnan University

(P.O. Box 35195-363, Semnan, Iran; e-mail: hmehraban@semnan.ac.ir, amin_asadi66@yahoo.com)

**FINAL STATE INTERACTION
EFFECTS IN $B^0 \rightarrow D^{0*} \bar{D}^0$ DECAY**

PACS 13.25.HW

The exclusive decay of $B^0 \rightarrow D^{0} \bar{D}^0$ is calculated by the QCD factorization (QCDF) method and a method involving the final state interaction (FSI). The result obtained by the QCDF method was less than the experimental value, which indicates the necessity to consider FSI. For the decay, the $D^+ D^{*-}$, $K^{+*} K^-$, $\rho^+ \pi^-$, $\rho^0 \pi^0$, $D_s^{*-} D_s^+$, and $J/\psi \pi^0$ via the exchange of π^- (ρ^-), D_s^- (D_s^{*-}), D^- (D^{*-}), \bar{D}^0 (\bar{D}^{0*}), and K^- (K^{*-}) mesons are chosen as intermediate states, which were calculated by the QCDF method. As for the FSI effects, the results of our calculations depend on η as the phenomenological parameter. The range of this parameter is selected to be from 0.8 to 1.6. If $\eta = 1.4$ is selected, the theoretical result fits the experimental branching ratio of the $B^0 \rightarrow D^{0*} \bar{D}^0$ decay that is less than 2.9×10^{-4} . Our results calculated by the QCDF and FSI methods are $(0.13 \pm 0.11) \times 10^{-4}$ and $(2.2 \pm 0.08) \times 10^{-4}$, respectively.*

Key words: B meson, QCD factorization, final state interaction, intermediate states, branching ratio.

1. Introduction

The importance of FSI in weak non-leptonic B meson decays is investigated, by using a relativistic chiral unitary approach based on coupled channels [1–3]. The chiral Lagrangian approach is proved to be reliable for evaluating the hadronic processes, but there are too many free parameters, which are determined by fitting data, so that its applications are much constrained. Therefore, we have tried to look for some simplified models, which can give rise to a reasonable estimation of FSI [4, 5]. The FSI can be considered as a re-scattering process of some intermediate two-body states with one-particle exchange in the t -channel and computed via the absorptive part of the hadronic loop level (HLL) diagrams. The calculation with the single-meson-exchange scenario is obviously much simpler and straightforward. Moreover, some theoretical uncertainties are included in an off-shell form factor, which modifies the effective vertices. Since the particle exchanged in the t -channel

is off shell, and since final state particles are hard, the form factors or cutoffs must be introduced to the strong vertices to render the calculation meaningful in perturbation theory. If the intermediate two-body mesons are hard enough, so that the perturbative calculation can make sense and work perfectly well, but the FSI can be modelled as the soft re-scattering of intermediate mesons. When one or two intermediate mesons can reach a low-energy region, where they are not sufficiently hard, one can be convinced that the perturbative QCD approach fails at this region or cannot result in reasonable values. If the intermediate mesons are soft, one can conjecture that, at this region, the non-perturbative QCD would dominate, and it could be attributed into the FSI effects. Because all FSI processes are concerning non-perturbative QCD [6], we have to rely on phenomenological models to analyze the FSI effects in certain reactions. In fact, after the weak decays of heavy mesons, the particles produced can re-scatter into other particle states through the non-perturbative strong interaction. We calculated the $B^0 \rightarrow D^{0*} \bar{D}^0$ decay according to the

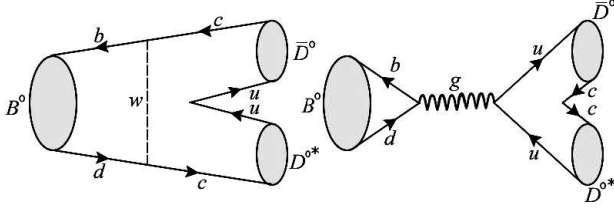


Fig. 1. Some quark diagrams illustrating the process $B^0 \rightarrow D^{0*} \bar{D}^0$

QCDF method and selected the leading order Wilson coefficients at the scale m_b and obtained the $\text{BR}(B^0 \rightarrow D^{0*} \bar{D}^0) = (0.13 \pm 0.11) \times 10^{-4}$. The FSI can give sizable corrections. The re-scattering amplitude can be derived by calculating the absorptive part of triangle diagrams. In this case, the intermediate states are $D^+ D^{*-}$, $K^{+*} K^-$, $\rho^+ \pi^-$, $\rho^0 \pi^0$, $D_s^{*-} D_s^+$, and $J/\psi \pi^0$. Then we calculated the $B^0 \rightarrow D^{0*} \bar{D}^0$ decay according to the HLL method. Taken FSI corrections into account, the branching ratio of $B^0 \rightarrow D^{0*} \times \bar{D}^0$ becomes $(2.2 \pm 0.08) \times 10^{-4}$, while the experimental result for this decay is less than 2.9×10^{-4} [7].

This paper is organized as follows. We present the QCDF calculation for $B^0 \rightarrow D^{0*} \bar{D}^0$ decay in Section 2. In Section 3, we calculate the amplitudes of the intermediate states of $B^0 \rightarrow D^+ D^{*-}$, $B^0 \rightarrow K^{+*} K^-$, $B^0 \rightarrow \rho^+ \pi^-$, $B^0 \rightarrow \rho^0 \pi^0$, $B^0 \rightarrow D_s^{*-} D_s^+$, and $B^0 \rightarrow J/\psi \pi^0$ decays. Then we present the HLL calculation for the $B^0 \rightarrow D^{0*} \bar{D}^0$ decay in Section 4. In Section 5, we give the numerical results, and in the last section, we have drawn a short conclusion.

2. QCD Factorization of $B^0 \rightarrow D^{0*} \bar{D}^0$ Decay

To compare QCDF with FSI, we explore QCDF analysis. In this case, we only have the current-current, penguin and electroweak penguin, annihilation effects. These contributions are small, but it is interesting and necessary to discuss them. For the annihilation amplitude, when all the equations for basic building blocks are solved, it is found that the weak annihilation kernels exhibit the endpoint divergence. Divergence terms are determined by $\int_0^1 dx/\bar{x}$ and $\int_0^1 dy/\bar{y}$. For the liberation of the divergence, a small ϵ of the Λ_{QCD}/M_B order was added to the denominator. So, the answer to the integral takes the $\ln(1+\epsilon)/\epsilon$ form, which is shown with X_A . Specifically, we treat X_A as a universal parameter obtained by using $\rho_A = 0.5$ and a strong phase for VP ($M_1 M_2$) case,

864

$\phi_A = -70^\circ$ [8]. According to Fig. 1, we obtained the annihilation amplitude as

$$A(B^0 \rightarrow D^{0*} \bar{D}^0) = i \frac{G_F}{\sqrt{2}} f_B f_D f_{D^*} (b_1 + 2b_4 + 2b_{4eW}), \quad (1)$$

where λ_p are the products of elements of the quark mixing matrix. Using the unitarity relation $\lambda_p + \lambda_c + \lambda_t = 0$, we write

$$\lambda_p = \sum_{p=u,c} V_{pb} V_{pd}^*, \quad (2)$$

and b_1 , b_4 , and b_{4eW} correspond to the current-current annihilation, penguin annihilation, and electroweak penguin annihilation. These non-singlet annihilation coefficients are given as

$$\begin{aligned} b_1 &= \frac{C_F}{N_c^2} c_1 A_1^i, \\ b_4 &= \frac{C_F^2}{N_c^2} [c_4 A_1^i + c_6 A_2^i], \\ b_{4,EW} &= \frac{C_F}{N_c^2} [c_1 0 A_1^i + c_8 A_2^i], \end{aligned} \quad (3)$$

where c_i are the Wilson coefficients, N_c is the color number, and

$$A_1^i \approx -A_2^i = 2\pi\alpha_s \left[9 \left(X_A - 4 + \frac{\pi^2}{3} \right) + r_\chi^D r_\chi^{D^*} X_A^2 \right], \quad (4)$$

$$C_F = \frac{N_c^2 - 1}{2N_c}.$$

For \bar{D}^0 and D^{0*} , the ratios are defined as

$$\begin{aligned} r_\chi^{\bar{D}^0} &= \frac{2m_{\bar{D}^0}^2}{(m_b - m_u)(m_c + m_u)}, \\ r_\chi^{D^{0*}} &= \frac{2m_{D^{0*}} f_{D^{0*}}^\perp}{m_b f_{D^{0*}}}. \end{aligned} \quad (5)$$

3. Amplitudes of Intermediate States

For the $B^0 \rightarrow D^+ D^{*-}$, $B^0 \rightarrow K^{+*} K^-$, $B^0 \rightarrow \rho^+ \pi^-$, $B^0 \rightarrow \rho^0 \pi^0$, $B^0 \rightarrow D_s^{*-} D_s^+$, and $B^0 \rightarrow J/\psi \pi^0$ decay amplitudes, we use

$$\begin{aligned} A(B^0 \rightarrow D^+ D^{*-}) &= -i\sqrt{2} G_F f_D m_{D^*} (\varepsilon_{D^*} \cdot p_B) A_0^{BD^*} \times \\ &\times \{ (a_1 + a_2) V_{cb} V_{cd}^* + [a_4 + a_1 0 + r_\psi^D (a_6 + a_8)] \lambda_p \} + \\ &+ i \frac{G_F}{\sqrt{2}} f_B f_D f_{D^*} \left\{ b_1 V_{cb} V_{cd}^* + \right. \\ &\left. + \left[b_3 + 2b_4 - \frac{1}{2} b_{3eW} + \frac{1}{2} b_{4eW} \right] \lambda_p \right\}, \end{aligned} \quad (6)$$

where

$$b_3 = \frac{c_F}{N_c^2} [c_3 A_1^i + c_5 (A_3^i + A_3^f) + N_c c_6 A_3^f],$$

$$b_{3,EW} = \frac{c_F}{N_c^2} [c_9 A_1^i + c_7 (A_3^i + A_3^f) + N_c c_8 A_3^f].$$

Here,

$$A_3^i = 0, \quad A_3^f = 2\pi\alpha_s (r_\chi^D + r_\chi^{D^*}) (2X_A^2 - X_A),$$

and

$$A(B^0 \rightarrow K^{+*} K^-) = +i \frac{G_F}{\sqrt{2}} f_B f_D f_{D^*} \times$$

$$\times \left\{ b_1 V_{cb} V_{cd}^* + \left[b_3 + 2b_4 - \frac{1}{2} b_{3eW} + \frac{1}{2} b_{4eW} \right] \lambda_p \right\},$$

$$A(B^0 \rightarrow \rho^+ \pi^-) = -i\sqrt{2} G_F f_\pi m_\rho (\varepsilon_\rho \cdot p_B) A_0^{B\rho} \times$$

$$\times \left\{ (a_1 + a_2) V_{ub} V_{ud}^* + \frac{1}{2} \left[a_4 + a_1 0 + r_\chi^\rho \left(a_6 - \frac{1}{2} a_8 \right) \right] \lambda_p \right\} +$$

$$+ i \frac{G_F}{\sqrt{2}} f_B f_\pi f_\rho \left\{ b_1 V_{ub} V_{ud}^* + \right.$$

$$\left. + \left[b_3 + 2b_4 + \frac{1}{2} b_{3eW} + \frac{1}{2} b_{4eW} \right] \lambda_p \right\},$$

where

$$r_\chi^\rho = \frac{2m_\rho}{m_b} \frac{f_\rho^\perp}{f_\rho},$$

and

$$A(B^0 \rightarrow \rho^0 \pi^0) = -i\sqrt{2} G_F f_\pi m_\rho (\varepsilon_\rho \cdot p_B) A_0^{B\rho} \times$$

$$\times \left\{ a_2 V_{ub} V_{ud}^* + \left[a_4 - \frac{1}{2} a_1 0 + \frac{3}{2} (a_7 - a_9) \times \right. \right.$$

$$\left. \times r_\chi^\rho \left(a_6 - \frac{1}{2} a_8 \right) \right] \lambda_p \right\} + i \frac{G_F}{\sqrt{2}} f_B f_\pi f_\rho \left\{ b_1 V_{ub} V_{ud}^* + \right.$$

$$\left. + \left[b_3 + 2b_4 - \frac{1}{2} b_{3eW} + \frac{1}{2} b_{4eW} \right] \lambda_p \right\}.$$

$$A(B^0 \rightarrow D_s^-^* D_s^+) = i \frac{G_F}{\sqrt{2}} f_B f_{D_s} f_{D_s^*} \times$$

$$\times \left\{ b_1 V_{cb} V_{cd}^* + \left[2b_4 + \frac{1}{2} b_{4eW} \right] \lambda_p \right\}.$$

$$A(B^0 \rightarrow J/\psi \pi^0) =$$

$$= -i\sqrt{2} G_F m_{J/\psi} (\varepsilon_{J/\psi} \cdot p_B) f_D A_0^{B \rightarrow J/\psi} \times$$

$$\times \{ V_{cb} V_{cd}^* a_2 + \lambda_p [a_3 + r_\chi^{J/\psi} (a_5 + a_7 + a_9)] \},$$

where

$$r_\chi^{J/\psi} = \frac{2m_{J/\psi}}{m_b} \frac{f_{J/\psi}^\perp}{f_{J/\psi}}.$$

4. Final State Interaction of the $B^0 \rightarrow D^{0*} \bar{D}^0$ Decay

For $B^0 \rightarrow D^{0*} \bar{D}^0$ decay, two-body intermediate states such as $D^+ D^{*-}$, $K^{+*} K^-$, $\rho^+ \pi^-$, $\rho^0 \pi^0$, $D_s^-^* D_s^+$, and $J/\psi \pi^0$ are produced. We can write out the decay amplitude involving HLL contributions with the formula

$$\text{Abs}M(B(p_B) \rightarrow M(p_1)M(p_2) \rightarrow M(p_3)M(p_4)) =$$

$$= \frac{1}{2} \int \frac{d^3 \mathbf{p}_1}{2E_1 (2\pi)^3} \frac{d^3 \mathbf{p}_2}{2E_2 (2\pi)^3} (2\pi)^4 \delta^4(p_B - p_1 - p_2) \times$$

$$\times M(B \rightarrow M_1 M_2) G(M_1 M_2 \rightarrow M_3 M_4),$$

for which both intermediate mesons (M_1, M_2) are pseudoscalar. The absorptive part of the HLL diagrams for the VP case can be calculated as

$$\text{Abs}M(B(p_B) \rightarrow M(p_1)M(p_2) \rightarrow M(p_3)M(p_4)) =$$

$$= \frac{1}{2} \int \frac{d^3 \mathbf{p}_1}{2E_1 (2\pi)^3} \frac{d^3 \mathbf{p}_2}{2E_2 (2\pi)^3} (2\pi)^4 \delta^4(p_B - p_1 - p_2) V_{\text{CKM}} \times$$

$$\times \{ 2a_i m_V (\varepsilon_V^* \cdot p_B) (f_p A_0^{B \rightarrow V} + f_V F_1^{B \rightarrow P}) +$$

$$+ f_B f_P f_V b_i \} G(M_1 M_2 \rightarrow M_3 M_4),$$

where $M(B \rightarrow M_1 M_2)$ is the amplitude of the $B \rightarrow M_1 M_2$ decay that is calculated via the QCDF method, and $G(M_1 M_2 \rightarrow M_3 M_4)$ involves the hadronic vertex factor defined as

$$\langle D^*(\varepsilon_3, p_3) \pi(p_2) | i \mathcal{L} | D(p_1) \rangle =$$

$$= -i g_{D_s^* K D} \varepsilon_3 \cdot (p_1 + p_2),$$

$$\langle D^*(\varepsilon_3, p_3) \rho(\varepsilon_2, p_2) | i \mathcal{L} | D(p_1) \rangle =$$

$$= -i\sqrt{2} g_{D^* D_s K^*} \varepsilon_{\mu\nu\alpha\beta} \varepsilon_2^\mu \varepsilon_3^{\nu} p_1^\alpha p_2^\beta.$$

The dispersive part of the re-scattering amplitude can be obtained from the absorptive part via the dispersion relation [6, 9]:

$$\text{Dis}M(m_B^2) = \frac{1}{\pi} \int_s^\infty \frac{\text{Abs}M(s')}{s' - m_B^2} ds',$$

where s' is the square of the momentum carried by the exchanged particle, and s is the threshold of intermediate states. In this case, $s \sim m_B^2$. Unlike the absorptive part, the dispersive contribution suffers from the large uncertainties arising from the complicated integration.

4.1. Final State Interaction in the $B^0 \rightarrow D^+ D^{*-} \rightarrow D^{0*} \bar{D}^0$ Decay

The quark model diagram for $B^0 \rightarrow D^+ D^{*-} \rightarrow D^{0*} \bar{D}^0$ decay is shown in Fig. 2. The hadronic level diagrams are shown in Fig. 3.

The amplitude of the mode $B^0 \rightarrow D^+(p_1) \times D^{*-}(\varepsilon_2, p_2) \rightarrow D^{0*}(\varepsilon_3, p_3) \bar{D}^0(p_4)$ is given by

$$\begin{aligned} \text{Abs}(7a) &= \frac{-iG_F}{2\sqrt{2}} \times \\ &\times \int_{-1}^1 \frac{d^3\mathbf{P}_1}{2E_1(2\pi)^3} \frac{d^3\mathbf{P}_2}{2E_2(2\pi)^3} (2\pi)^4 \delta^4(p_B - p_1 - p_2) \times \\ &\times (-ig_{D^*KD}) \varepsilon_3 \cdot (p_1 + q) (-ig_{DKD^*}) \times \\ &\times \varepsilon_2 \cdot (-q) \left\{ 2m_{D^*} (\varepsilon_2 \cdot p_1) f_D A_0^{BD^*} \times \right. \\ &\times [(a_1 + a_2) V_{cb} V_{cd}^* + (a_4 + r_\chi^{D^*} (a_6 + a_8) + a_1 0) \lambda_p] - \\ &- f_B f_D f_{D^*} \left[b_1 V_{cb} V_{cd}^* + \right. \\ &\left. + \left(b_3 + 2b_4 - \frac{1}{2} b_{3eW} + \frac{1}{2} b_{4eW} \right) \lambda_p \right] \left. \right\} \frac{F^2(q^2, m_K^2)}{T_1}, \\ &= \frac{-iG_F}{8\sqrt{2}\pi m_B} g_{D^*KD} g_{DKD^*} \times \\ &\times \int_{-1}^1 |P_1| d(\cos\theta) \times \left\{ 2H_1 m_{D^*} f_D A_0^{BD^*} \times \right. \\ &\times [(a_1 + a_2) V_{cb} V_{cd}^* + (a_4 + r_\chi^{D^*} (a_6 + a_8) + a_1 0) \lambda_p] - \\ &- f_B f_D f_{D^*} \left[b_1 V_{cb} V_{cd}^* + \left(b_3 + 2b_4 - \frac{1}{2} b_{3eW} + \right. \right. \end{aligned}$$

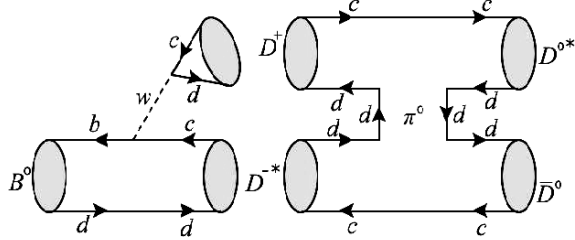


Fig. 2. Quark level diagram for $B^0 \rightarrow D^+ D^{*-}$

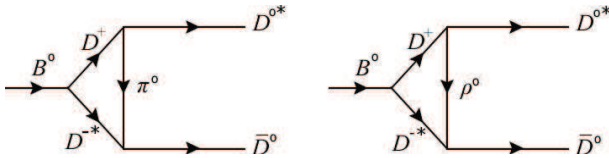


Fig. 3. HLL diagrams for the long-distance t -channel contribution to $B^0 \rightarrow D^{0*} \bar{D}^0$

$$\left. + \frac{1}{2} b_{4eW} \right] \lambda_p \left. \right\} \frac{F^2(q^2, m_K^2)}{T_1}, \quad (20)$$

where

$$\begin{aligned} H_1 &= (\varepsilon_2 \cdot p_1)(\varepsilon_2 \cdot p_4)(\varepsilon_3 \cdot p_1) = \\ &= \left(-p_1 \cdot p_4 + \frac{(p_1 \cdot p_2)(p_2 \cdot p_4)}{m_{D^*}^2} \right) \left(\frac{E_1 |p_3| - E_3 |p_1| \cos\theta}{m_B |p_3|} \right), \\ H_2 &= (\varepsilon_3 \cdot p_1)(\varepsilon_2 \cdot p_4) = \\ &= \left(\frac{E_1 |p_3| - E_3 |p_1| \cos\theta}{m_B |p_3|} \right) \left(\frac{E_4 |p_2| - E_2 |p_4| \cos\theta}{m_B |p_2|} \right), \quad (21) \\ T_1 &= (p_1 - p_3)^2 - m_K^2 = p_1^2 + p_3^2 - 2p_1^0 p_3^0 + 2\mathbf{p}_1 \cdot \mathbf{p}_3 - m_K^2, \\ q^2 &= m_1^2 + m_3^2 - 2E_1 E_3 + 2|\mathbf{p}_1||\mathbf{p}_3| \cos\theta = \\ &= m_D^2 + m_{D^*}^2 - 2p_1^0 p_3^0 + 2|\mathbf{p}_1||\mathbf{p}_3| \cos\theta, \end{aligned}$$

θ is the angle between \mathbf{p}_1 and \mathbf{p}_3 , q is the momentum of the exchange K^0 meson, and $F(q^2, m_K^2)$ is the form factor defined to take care of the off-shell of the exchange particles, which is introduced as [1, 10]

$$F(q^2, m_D^2) = \left(\frac{\Lambda^2 - m_K^2}{\Lambda^2 - q^2} \right)^n. \quad (22)$$

The form factor (i.e. $n = 1$) normalized to 1 at $q^2 = m_K^2$. The quantities m_K and q are the physical parameters of the exchange particle, and Λ is a phenomenological parameter. It is obvious that, as $q^2 \rightarrow 0$, $F(q^2, m_K^2)$ becomes a number. If $\Lambda \gg m_K$, then $F(q^2, m_K^2)$ turns to be 1, whereas, as $q^2 \rightarrow \infty$, the form factor approaches zero, the distance becomes small, and the hadron interaction is no longer valid. Since Λ should not be far from m_K and q , we choose

$$\Lambda = m_K + \eta \Lambda_{\text{QCD}}, \quad (23)$$

where the η is the phenomenological parameter. Its value in the form factor is expected to be of the order of 1 and can be determined from the measured rates, and

$$\text{Abs}(7b) = \frac{-iG_F}{2\sqrt{2}} \times$$

$$\begin{aligned} &\int_{-1}^1 \frac{d^3\mathbf{P}_1}{2E_1(2\pi)^3} \frac{d^3\mathbf{P}_2}{2E_2(2\pi)^3} (2\pi)^4 \delta^4(p_B - p_1 - p_2) \times \\ &\times (-i\sqrt{2}g_{DK^*D^*}) \varepsilon_{\mu\nu\alpha\beta} \varepsilon_3^\mu \varepsilon_{K^*}^\nu p_1^\alpha p_3^\beta (-i\sqrt{2}g_{D^*K^*D}) \times \\ &\times \varepsilon_{\rho\sigma\lambda\eta} \varepsilon_2^\rho \varepsilon_{K^*}^\sigma p_2^\lambda p_4^\eta \left\{ 2m_{D^*} (\varepsilon_2 \cdot p_1) f_D A_0^{BD^*} \times \right. \\ &\times [(a_1 + a_2) V_{cb} V_{cd}^* + (a_4 + r_\chi^{D^*} (a_6 + a_8) + a_1 0) \lambda_p] - \end{aligned}$$

$$\begin{aligned}
 & -f_B f_D f_{D^*} \left[b_1 V_{cb} V_{cd}^* + \right. \\
 & \left. + \left(b_3 + 2b_4 - \frac{1}{2} b_{3eW} + \frac{1}{2} b_{4eW} \right) \lambda_p \right] \frac{F^2(q^2, m_{K^*}^2)}{T_2} = \\
 & = \frac{iG_F}{8\sqrt{2}\pi m_B} g_{DK^*D^*} g_{D^*K^*D} \int_{-1}^1 |P_1| d(\cos\theta) \times \\
 & \times \left\{ 2H_3 m_{D^*} (\varepsilon_2 \cdot p_1) f_D A_0^{BD^*} \left[(a_1 + a_2) V_{cb} V_{cd}^* + \right. \right. \\
 & \left. \left. + (a_4 + r_\chi^{D^*} (a_6 + a_8) + a_{10}) \lambda_p \right] - \right. \\
 & \left. - f_B f_D f_{D^*} \left[b_1 V_{cb} V_{cd}^* + \left(b_3 + 2b_4 - \frac{1}{2} b_{3eW} + \right. \right. \right. \\
 & \left. \left. \left. + \frac{1}{2} b_{4eW} \right) \lambda_p \right] H_4 \right\} \frac{F^2(q^2, m_{K^*}^2)}{T_2}, \quad (24)
 \end{aligned}$$

where

$$\begin{aligned}
 H_3 & = m_3^2 (p_1 \cdot p_2) - (p_1 \cdot p_3)(p_2 \cdot p_3) + \\
 & + \left(\frac{E_2 |p_3| - E_3 |p_2| \cos\theta}{m_B |p_3|} \right) \times \\
 & \times [(p_B \cdot p_1)(p_3 \cdot p_4) - (p_B \cdot p_3)(p_1 \cdot p_4)], \\
 H_4 & = \varepsilon_{\mu\nu\lambda\beta} \varepsilon_{\rho\sigma\lambda\eta} \varepsilon_3^\mu \varepsilon_{K^*}^\nu p_1^\alpha p_3^\beta \varepsilon_2^\rho \varepsilon_{K^*}^\sigma p_2^\lambda p_4^\eta, \\
 T_2 & = (p_1 - p_3)^2 - m_{K^*}^2 = p_1^2 + p_3^2 - \\
 & - 2p_1^0 p_3^0 + 2\mathbf{p}_1 \cdot \mathbf{p}_3 - m_{K^*}^2, \\
 q^2 & = m_1^2 + m_3^2 - 2E_1 E_3 + 2|\mathbf{p}_1||\mathbf{p}_3| \cos\theta = \\
 & = m_D^2 + m_{D^*}^2 - 2p_1^0 p_3^0 + 2|\mathbf{p}_1||\mathbf{p}_3| \cos\theta.
 \end{aligned} \quad (25)$$

The dispersion relation is

$$\text{Dis}3(m_B^2) = \frac{1}{\pi} \int_s^\infty \frac{\text{Abs}3a(s') + \text{Abs}3b(s')}{s' - m_B^2} ds'. \quad (26)$$

4.2. Final State Interaction in the $B^0 \rightarrow K^{+*} K^- \rightarrow D^{0*} \bar{D}^0$ Decay

The quark model diagram for $B^0 \rightarrow K^{+*} K^- \rightarrow D^{0*} \bar{D}^0$ decay is shown in Fig. 4, and the hadronic level diagrams are shown in Fig. 5. We have

$$\begin{aligned}
 \text{Abs}(5a) & = \frac{-iG_F}{2\sqrt{2}} \int_{-1}^1 \frac{d^3\mathbf{P}_1}{2E_1(2\pi)^3} \frac{d^3\mathbf{P}_2}{2E_2(2\pi)^3} \times \\
 & \times (2\pi)^4 \delta^4(p_B - p_1 - p_2) \times \\
 & \times (-ig_{KKD^*}) \varepsilon_3 \cdot (p_1 + q) (-ig_{K^*KD}) \varepsilon_2 \cdot (-q) f_B f_K f_{K^*} \times
 \end{aligned}$$

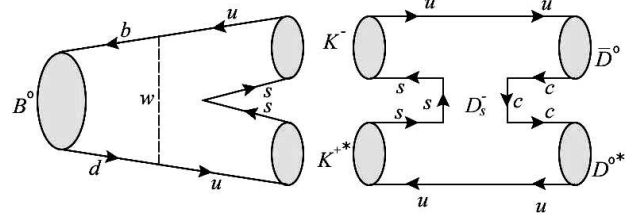


Fig. 4. Quark level diagram for $B^0 \rightarrow K^{+*} K^-$

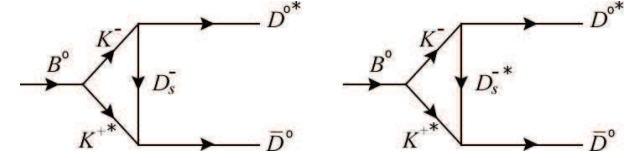


Fig. 5. HLL diagrams for the long-distance t -channel contribution to $B^0 \rightarrow D^{0*} D^0$

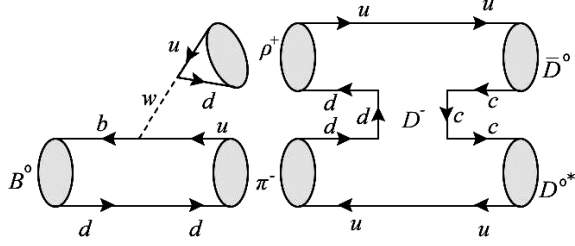
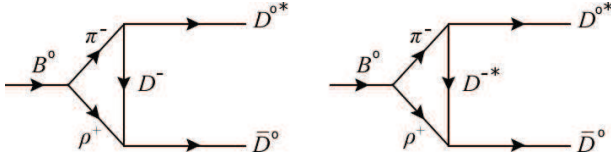
$$\begin{aligned}
 & \times \left[b_1 V_{ub} V_{ud}^* + \left(2b_4 + \frac{1}{2} b_{4eW} \right) \right] \lambda_p \frac{F^2(q^2, m_{D_s}^2)}{T_1} = \\
 & = \frac{-iG_F}{8\sqrt{2}\pi m_B} g_{KKD^*} g_{K^*KD} \int_{-1}^1 |P_1| d(\cos\theta) \times \\
 & \times f_B f_K f_{K^*} \left[b_1 V_{ub} V_{ud}^* + \left(2b_4 + \frac{1}{2} b_{4eW} \right) \right] \times \\
 & \times \lambda_p \frac{F^2(q^2, m_{D_s}^2)}{T_1} H_1, \quad (27)
 \end{aligned}$$

where

$$\begin{aligned}
 H_1 & = (\varepsilon_3 \cdot p_1)(\varepsilon_2 \cdot p_4) = \\
 & = \left(\frac{E_1 |p_3| - E_3 |p_1| \cos\theta}{m_B |p_3|} \right) \left(\frac{E_4 |p_2| - E_2 |p_4| \cos\theta}{m_B |p_2|} \right), \\
 T_1 & = (p_1 - p_3)^2 - m_{D_s}^2 = p_1^2 + p_3^2 - \\
 & - 2p_1^0 p_3^0 + 2\mathbf{p}_1 \cdot \mathbf{p}_3 - m_{D_s}^2, \\
 q^2 & = m_1^2 + m_3^2 - 2E_1 E_3 + 2|\mathbf{p}_1||\mathbf{p}_3| \cos\theta = \\
 & = m_K^2 + m_{D^*}^2 - 2p_1^0 p_3^0 + 2|\mathbf{p}_1||\mathbf{p}_3| \cos\theta,
 \end{aligned} \quad (28)$$

and

$$\begin{aligned}
 \text{Abs}(5b) & = \frac{-iG_F}{2\sqrt{2}} \int_{-1}^1 \frac{d^3\mathbf{P}_1}{2E_1(2\pi)^3} \frac{d^3\mathbf{P}_2}{2E_2(2\pi)^3} \times \\
 & \times (2\pi)^4 \delta^4(p_B - p_1 - p_2) (-i\sqrt{2} g_{KK^*D^*}) \times \\
 & \times \varepsilon_{\mu\nu\alpha\beta} \varepsilon_3^\mu \varepsilon_{K^*}^\nu p_1^\alpha p_3^\beta (-i\sqrt{2} g_{K^*K^*D}) \varepsilon_{\rho\sigma\lambda\eta} \varepsilon_2^\rho \varepsilon_{K^*}^\sigma p_2^\lambda p_4^\eta \times \\
 & \times f_B f_K f_{K^*} \left[b_1 V_{ub} V_{ud}^* + \left(2b_4 + \frac{1}{2} b_{4eW} \right) \right] \times \\
 & \times \lambda_p \frac{F^2(q^2, m_{D_s}^2)}{T_2} = \frac{iG_F}{8\sqrt{2}\pi m_B} g_{KK^*D^*} g_{K^*K^*D} \times
 \end{aligned}$$


Fig. 6. Quark level diagram for $B^0 \rightarrow \rho^+ \pi^-$

Fig. 7. HLL diagrams for the long-distance t -channel contribution to $B^0 \rightarrow D^{0*} \bar{D}^0$

$$\begin{aligned} & \times \int_{-1}^1 |P_1| d(\cos \theta) f_B f_K f_{K^*} \left[b_1 V_{ub} V_{ud}^* + \left(2b_4 + \frac{1}{2} b_{4eW} \right) \right] \times \\ & \times \lambda_p \frac{F^2(q^2, m_{D_s^*}^2)}{T_2} H_2, \end{aligned} \quad (29)$$

where

$$\begin{aligned} H_2 &= \varepsilon_{\mu\nu\alpha\beta} \varepsilon_{\rho\sigma\lambda\eta} \varepsilon_3^\mu \varepsilon_{K^*}^\nu p_1^\alpha p_3^\beta \varepsilon_2^\rho \varepsilon_{K^*}^\sigma p_2^\lambda p_4^\eta, \\ T_2 &= (p_1 - p_3)^2 - m_{D_s^*}^2 = p_1^2 + p_3^2 - \\ & - 2p_1^0 p_3^0 + 2\mathbf{p}_1 \cdot \mathbf{p}_3 - m_{D_s^*}^2, \\ q^2 &= m_1^2 + m_3^2 - 2E_1 E_3 + 2|\mathbf{p}_1| |\mathbf{p}_3| \cos \theta = \\ & = m_K^2 + m_{D^*}^2 - 2p_1^0 p_3^0 + 2|\mathbf{p}_1| |\mathbf{p}_3| \cos \theta. \end{aligned} \quad (30)$$

The dispersion relation is

$$\text{Dis}5(m_B^2) = \frac{1}{\pi} \int_s^\infty \frac{\text{Abs}5a(s') + \text{Abs}5b(s')}{s' - m_B^2} ds'. \quad (31)$$

4.3. Final State Interaction in the $B^0 \rightarrow \rho^+ \pi^- \rightarrow D^{0*} \bar{D}^0$ Decay

The quark model diagram for $B^0 \rightarrow \rho^+ \pi^- \rightarrow D^{0*} \bar{D}^0$ decay is shown in Fig. 6, and the hadronic level diagrams are shown in Fig. 7. We have

$$\begin{aligned} \text{Abs}(7a) &= \frac{-iG_F}{2\sqrt{2}} \int_{-1}^1 \frac{d^3 \mathbf{P}_1}{2E_1 (2\pi)^3} \frac{d^3 \mathbf{P}_2}{2E_2 (2\pi)^3} \times \\ & \times (2\pi)^4 \delta^4(p_B - p_1 - p_2) (-ig_{\pi D D^*}) \varepsilon_3 \cdot (p_1 + q) (-ig_{\rho D D}) \times \end{aligned}$$

$$\begin{aligned} & \times \varepsilon_2 \cdot (-q) \left\{ 2m_\rho (\varepsilon_2 \cdot p_1) f_\pi A_0^{B\rho} \left[(a_1 + a_2) V_{ub} V_{ud}^* + \right. \right. \\ & \left. \left. + \frac{1}{2} \left(a_4 + r_\chi^\rho \left(a_6 - \frac{1}{2} a_8 \right) + a_{10} \right) \lambda_p \right] - f_B f_\pi f_\rho \times \right. \\ & \left. \times \left[b_1 V_{ub} V_{ud}^* + \left(b_3 + 2b_4 + \frac{1}{2} b_{3eW} + \right. \right. \right. \\ & \left. \left. \left. + \frac{1}{2} b_{4eW} \right) \lambda_p \right] \right\} \frac{F^2(q^2, m_D^2)}{T_1}, \\ & = \frac{-iG_F}{8\sqrt{2}\pi m_B} g_{\pi D D^*} g_{\rho D D} \times \\ & \times \int_{-1}^1 |P_1| d(\cos \theta) \left\{ 2H_1 m_\rho f_\pi A_0^{B\rho} \left[(a_1 + a_2) \times \right. \right. \\ & \left. \left. \times V_{ub} V_{ud}^* + \frac{1}{2} \left(a_4 + r_\chi^\rho \left(a_6 - \frac{1}{2} a_8 \right) + a_{10} \right) \lambda_p \right] - \right. \\ & \left. - f_B f_\pi f_\rho \left[b_1 V_{ub} V_{ud}^* + \left(b_3 + 2b_4 + \frac{1}{2} b_{3eW} + \right. \right. \right. \\ & \left. \left. \left. + \frac{1}{2} b_{4eW} \right) \lambda_p \right] H_2 \right\} \frac{F^2(q^2, m_D^2)}{T_1}, \end{aligned} \quad (32)$$

where

$$\begin{aligned} (H)_1 &= (\varepsilon_2 \cdot p_1) (\varepsilon_2 \cdot p_4) (\varepsilon_3 \cdot p_1) = \\ & = \left(-p_1 \cdot p_4 + \frac{(p_1 \cdot p_2)(p_2 \cdot p_4)}{m_\rho^2} \right) \left(\frac{E_1 |p_3| - E_3 |p_1| \cos \theta}{m_B |p_3|} \right), \\ H_2 &= (\varepsilon_3 \cdot p_1) (\varepsilon_2 \cdot p_4) = \\ & = \left(\frac{E_1 |p_3| - E_3 |p_1| \cos \theta}{m_B |p_3|} \right) \left(\frac{E_4 |p_2| - E_2 |p_4| \cos \theta}{m_B |p_2|} \right), \end{aligned} \quad (33)$$

$$\begin{aligned} T_1 &= (p_1 - p_3)^2 - m_D^2 = p_1^2 + p_3^2 - \\ & - 2p_1^0 p_3^0 + 2\mathbf{p}_1 \cdot \mathbf{p}_3 - m_D^2, \\ q^2 &= m_1^2 + m_3^2 - 2E_1 E_3 + 2|\mathbf{p}_1| |\mathbf{p}_3| \cos \theta = \\ & = m_\pi^2 + m_{D^*}^2 - 2p_1^0 p_3^0 + 2|\mathbf{p}_1| |\mathbf{p}_3| \cos \theta, \end{aligned}$$

and

$$\begin{aligned} \text{Abs}(7b) &= \frac{-iG_F}{2\sqrt{2}} \int_{-1}^1 \frac{d^3 \mathbf{P}_1}{2E_1 (2\pi)^3} \frac{d^3 \mathbf{P}_2}{2E_2 (2\pi)^3} (2\pi)^4 \times \\ & \times \delta^4(p_B - p_1 - p_2) (-ig_{\pi D^* D^*}) \varepsilon_3 \cdot (p_1 + q) (-ig_{\rho D^* D}) \times \\ & \times \varepsilon_2 \cdot (-q) \left\{ 2m_\rho (\varepsilon_2 \cdot p_1) f_\pi A_0^{B\rho} \left[(a_1 + a_2) V_{ub} V_{ud}^* + \right. \right. \\ & \left. \left. + \frac{1}{2} \left(a_4 + r_\chi^\rho \left(a_6 - \frac{1}{2} a_8 \right) + a_{10} \right) \lambda_p \right] - f_B f_\pi f_\rho \times \right. \\ & \left. \times \left[b_1 V_{ub} V_{ud}^* + \left(b_3 + 2b_4 + \frac{1}{2} b_{3eW} + \right. \right. \right. \end{aligned}$$

$$\begin{aligned}
 & + \frac{1}{2} b_{4eW} \lambda_p \left. \right\} \frac{F^2(q^2, m_{D^*}^2)}{T_2}, \\
 & = \frac{-iG_F}{8\sqrt{2}\pi m_B} g_{\pi D^* D^*} g_{\rho D^* D} \int_{-1}^1 |P_1| d(\cos \theta) \times \\
 & \times \left\{ 2H_3 m_\rho f_\pi A_0^{B\rho} \left[(a_1 + a_2) V_{ub} V_{ud}^* + \frac{1}{2} \left(a_4 + r_\chi^\rho \times \right. \right. \right. \\
 & \times \left. \left. \left(a_6 - \frac{1}{2} a_8 \right) + a_{10} \right) \lambda_p \right] - f_B f_\pi f_\rho \left[b_1 V_{ub} V_{ud}^* + \right. \\
 & + \left. \left(b_3 + 2b_4 + \frac{1}{2} b_{3eW} + \frac{1}{2} b_{4eW} \right) \lambda_p \right] H_4 \right\} \times \\
 & \times \frac{F^2(q^2, m_{D^*}^2)}{T_2},
 \end{aligned}
 \tag{34}$$

where

$$\begin{aligned}
 H_3 & = m_3^2(p_1.p_2) - (p_1.p_3)(p_2.p_3) + \\
 & + \left(\frac{E_2|p_3| - E_3|p_2|\cos\theta}{m_B|p_3|} \right) \times \\
 & \times [(p_B.p_1)(p_3.p_4) - (p_B.p_3)(p_1.p_4)], \\
 H_4 & = \varepsilon_{\mu\nu\alpha\beta} \varepsilon_{\rho\sigma\lambda\eta} \varepsilon_3^\mu \varepsilon_{K^*}^\nu p_1^\alpha p_3^\beta \varepsilon_2^\rho \varepsilon_{K^*}^\sigma p_2^\lambda p_4^\eta, \\
 T_2 & = (p_1 - p_3)^2 - m_{D^*}^2 = \\
 & = p_1^2 + p_3^2 - 2p_1^0 p_3^0 + 2\mathbf{p}_1 \cdot \mathbf{p}_3 - m_{D^*}^2, \\
 q^2 & = m_1^2 + m_3^2 - 2E_1 E_3 + 2|\mathbf{p}_1||\mathbf{p}_3|\cos\theta = \\
 & = m_\pi^2 + m_{D^*}^2 - 2p_1^0 p_3^0 + 2|\mathbf{p}_1||\mathbf{p}_3|\cos\theta.
 \end{aligned}
 \tag{35}$$

The dispersion relation is

$$\text{Dis}7(m_B^2) = \frac{1}{\pi} \int_s^\infty \frac{\text{Abs}7a(s') + \text{Abs}7b(s')}{s' - m_B^2} ds'. \tag{36}$$

4.4. Final State Interaction in the $B^0 \rightarrow \rho^0 \pi^0 \rightarrow D^{0*} \bar{D}^0$ Decay

The quark model diagram for $B^0 \rightarrow \rho^0 \pi^0 \rightarrow D^{0*} \bar{D}^0$ decay is shown in Fig. 8, and the hadronic level diagrams are shown in Fig. 9. We have

$$\begin{aligned}
 \text{Abs}(9a) & = \frac{-iG_F}{2\sqrt{2}} \int_{-1}^1 \frac{d^3\mathbf{P}_1}{2E_1(2\pi)^3} \frac{d^3\mathbf{P}_2}{2E_2(2\pi)^3} (2\pi)^4 \times \\
 & \times \delta^4(p_B - p_1 - p_2) (-ig_{\pi DD^*}) \varepsilon_3.(p_1 + q) (-ig_{\rho DD}) \times \\
 & \times \varepsilon_2.(-q) \left\{ 2m_\rho (\varepsilon_2.p_1) f_\pi A_0^{B\rho} \left[a_2 V_{ub} V_{ud}^* + \right. \right. \\
 & + \left. \left. \left(a_4 + r_\chi^\rho \left(a_6 - \frac{1}{2} a_8 \right) - \frac{1}{2} a_{10} + \frac{3}{2} (a_7 - a_9) \right) \lambda_p \right] - \right.
 \end{aligned}$$

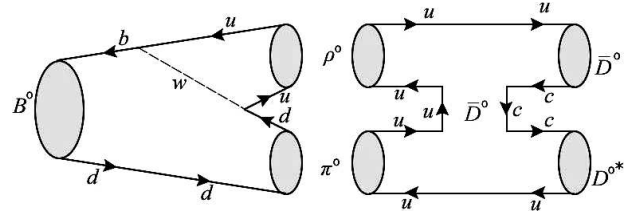


Fig. 8. Quark level diagram for $B^0 \rightarrow \rho^0 \pi^0$

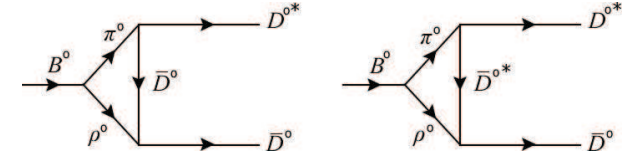
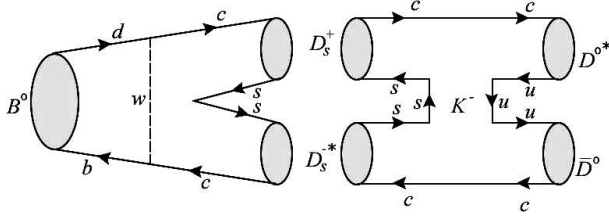
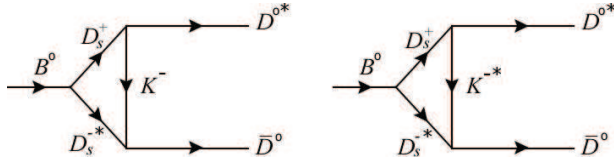


Fig. 9. HLL diagrams for the long-distance t -channel contribution to $B^0 \rightarrow D^{0*} \bar{D}^0$

$$\begin{aligned}
 & - f_B f_\pi f_\rho \left[b_1 V_{ub} V_{ud}^* + \left(b_3 + 2b_4 - \frac{1}{2} b_{3eW} + \right. \right. \\
 & + \left. \left. \frac{1}{2} b_{4eW} \right) \lambda_p \right] \left. \right\} \frac{F^2(q^2, m_D^2)}{T_1}, \\
 & = \frac{-iG_F}{8\sqrt{2}\pi m_B} g_{\pi DD^*} g_{\rho DD} \int_{-1}^1 |P_1| d(\cos \theta) \times \\
 & \times \left\{ 2H_1 m_\rho f_\pi A_0^{B\rho} \left[a_2 V_{ub} V_{ud}^* + \right. \right. \\
 & + \left. \left. \left(a_4 + r_\chi^\rho \left(a_6 - \frac{1}{2} a_8 \right) - \frac{1}{2} a_{10} + \frac{3}{2} (a_7 - a_9) \right) \lambda_p \right] \times \right. \\
 & - f_B f_\pi f_\rho \left[b_1 V_{ub} V_{ud}^* + \left(b_3 + 2b_4 - \frac{1}{2} b_{3eW} + \right. \right. \\
 & + \left. \left. \frac{1}{2} b_{4eW} \right) \lambda_p \right] H_2 \left. \right\} \frac{F^2(q^2, m_D^2)}{T_1}, \tag{37}
 \end{aligned}$$

where

$$\begin{aligned}
 H_1 & = (\varepsilon_2.p_1)(\varepsilon_2.p_4)(\varepsilon_3.p_1) = \\
 & = \left(-p_1.p_4 + \frac{(p_1.p_2)(p_2.p_4)}{m_\rho^2} \right) \left(\frac{E_1|p_3| - E_3|p_1|\cos\theta}{m_B|p_3|} \right), \\
 H_2 & = (\varepsilon_3.p_1)(\varepsilon_2.p_4) = \\
 & = \left(\frac{E_1|p_3| - E_3|p_1|\cos\theta}{m_B|p_3|} \right) \left(\frac{E_4|p_2| - E_2|p_4|\cos\theta}{m_B|p_2|} \right), \tag{38} \\
 T_1 & = (p_1 - p_3)^2 - m_D^2 = \\
 & = p_1^2 + p_3^2 - 2p_1^0 p_3^0 + 2\mathbf{p}_1 \cdot \mathbf{p}_3 - m_D^2, \\
 q^2 & = m_1^2 + m_3^2 - 2E_1 E_3 + 2|\mathbf{p}_1||\mathbf{p}_3|\cos\theta = \\
 & = m_\pi^2 + m_{D^*}^2 - 2p_1^0 p_3^0 + 2|\mathbf{p}_1||\mathbf{p}_3|\cos\theta.
 \end{aligned}$$


Fig. 10. Quark level diagram for $B^0 \rightarrow D_s^- D_s^+$

Fig. 11. HLL diagrams for the long-distance t -channel contribution to $B^0 \rightarrow D^{0*} \bar{D}^0$

and

$$\begin{aligned}
\text{Abs}(9b) &= \frac{-iG_F}{2\sqrt{2}} \int_{-1}^1 \frac{d^3\mathbf{P}_1}{2E_1(2\pi)^3} \frac{d^3\mathbf{P}_2}{2E_2(2\pi)^3} (2\pi)^4 \times \\
&\times \delta^4(p_B - p_1 - p_2) (-ig_{\pi D^* D^*}) \varepsilon_3 \cdot (p_1 + q) (-ig_{\rho D^* D}) \times \\
&\times \varepsilon_2 \cdot (-q) \left\{ 2m_\rho (\varepsilon_2 \cdot p_1) f_\pi A_0^{B\rho} \left[a_2 V_{ub} V_{ud}^* + \right. \right. \\
&+ \left. \left(a_4 + r_\chi^\rho \left(a_6 - \frac{1}{2} a_8 \right) - \frac{1}{2} a_{10} + \frac{3}{2} (a_7 - a_9) \right) \lambda_p \right] - \\
&- f_B f_\pi f_\rho \left[b_1 V_{ub} V_{ud}^* + \left(b_3 + 2b_4 - \frac{1}{2} b_{3eW} + \right. \right. \\
&+ \left. \left. \frac{1}{2} b_{4eW} \right) \lambda_p \right] \left. \right\} \frac{F^2(q^2, m_D^2)}{T_2}, \\
&= \frac{-iG_F}{8\sqrt{2}\pi m_B} g_{\pi D^* D^*} g_{\rho D^* D} \int_{-1}^1 |P_1| d(\cos \theta) \times \\
&\times \left\{ 2H_3 m_\rho f_\pi A_0^{B\rho} \left[a_2 V_{ub} V_{ud}^* + \right. \right. \\
&+ \left. \left(a_4 + r_\chi^\rho \left(a_6 - \frac{1}{2} a_8 \right) - \frac{1}{2} a_{10} + \frac{3}{2} (a_7 - a_9) \right) \lambda_p \right] - \\
&- f_B f_\pi f_\rho \left[b_1 V_{ub} V_{ud}^* + \left(b_3 + 2b_4 - \frac{1}{2} b_{3eW} + \right. \right. \\
&+ \left. \left. \frac{1}{2} b_{4eW} \right) \lambda_p \right] H_4 \left. \right\} \frac{F^2(q^2, m_D^2)}{T_2}, \quad (39)
\end{aligned}$$

870

where

$$\begin{aligned}
H_3 &= m_3^2 (p_1 \cdot p_2) - (p_1 \cdot p_3) (p_2 \cdot p_3) + \\
&+ \left(\frac{E_2 |p_3| - E_3 |p_2| \cos \theta}{m_B |p_3|} \right) \times \\
&\times [(p_B \cdot p_1) (p_3 \cdot p_4) - (p_B \cdot p_3) (p_1 \cdot p_4)], \\
H_4 &= \varepsilon_{\mu\nu\alpha\beta} \varepsilon_{\rho\sigma\lambda\eta} \varepsilon_3^\mu \varepsilon_{K^*}^\nu p_1^\alpha p_3^\beta \varepsilon_2^\rho \varepsilon_{K^*}^\sigma p_2^\lambda p_4^\eta, \quad (40) \\
T_2 &= (p_1 - p_3)^2 - m_D^2 = \\
&= p_1^2 + p_3^2 - 2p_1^0 p_3^0 + 2\mathbf{p}_1 \cdot \mathbf{p}_3 - m_D^2, \\
q^2 &= m_1^2 + m_3^2 - 2E_1 E_3 + 2|\mathbf{p}_1| |\mathbf{p}_3| \cos \theta = \\
&= m_\pi^2 + m_{D^*}^2 - 2p_1^0 p_3^0 + 2|\mathbf{p}_1| |\mathbf{p}_3| \cos \theta.
\end{aligned}$$

The dispersion relation is

$$\text{Dis}9(m_B^2) = \frac{1}{\pi} \int_s^\infty \frac{\text{Abs}9a(s') + \text{Abs}9b(s')}{s' - m_B^2} ds'. \quad (41)$$

4.5. Final State Interaction

in $B^0 \rightarrow D_s^- D_s^+ \rightarrow D^{0*} \bar{D}^0$ Decay

The quark model diagram for $B^0 \rightarrow D_s^- D_s^+ \rightarrow D^{0*} \bar{D}^0$ decay is shown in Fig. 10, and the hadronic level diagrams are shown in Fig. 11. We have

$$\begin{aligned}
\text{Abs}(11a) &= \frac{-iG_F}{2\sqrt{2}} \int_{-1}^1 \frac{d^3\mathbf{P}_1}{2E_1(2\pi)^3} \frac{d^3\mathbf{P}_2}{2E_2(2\pi)^3} (2\pi)^4 \times \\
&\times \delta^4(p_B - p_1 - p_2) (-ig_{D_s K D^*}) \varepsilon_3 \cdot (p_1 + q) (-ig_{D_s^* K D}) \times \\
&\times \varepsilon_2 \cdot (-q) f_B f_{D_s} f_{D_s^*} \left[b_1 V_{cb} V_{cd}^* + \right. \\
&+ \left. \left(2b_4 + \frac{1}{2} b_{4eW} \right) \lambda_p \frac{F^2(q^2, m_K^2)}{T_1} \right] \\
&= \frac{-iG_F}{8\sqrt{2}\pi m_B} g_{D_s K D^*} g_{D_s^* K D} \int_{-1}^1 |P_1| d(\cos \theta) f_B f_{D_s} f_{D_s^*} \times \\
&\times \left[b_1 V_{cb} V_{cd}^* + \left(2b_4 + \frac{1}{2} b_{4eW} \right) \lambda_p \frac{F^2(q^2, m_K^2)}{T_1} \right] H_1, \quad (42)
\end{aligned}$$

where

$$\begin{aligned}
H_1 &= (\varepsilon_3 \cdot p_1) (\varepsilon_2 \cdot p_4) = \\
&= \left(\frac{E_1 |p_3| - E_3 |p_1| \cos \theta}{m_B |p_3|} \right) \left(\frac{E_4 |p_2| - E_2 |p_4| \cos \theta}{m_B |p_2|} \right), \\
T_1 &= (p_1 - p_3)^2 - m_K^2 = \\
&= p_1^2 + p_3^2 - 2p_1^0 p_3^0 + 2\mathbf{p}_1 \cdot \mathbf{p}_3 - m_K^2, \\
q^2 &= m_1^2 + m_3^2 - 2E_1 E_3 + 2|\mathbf{p}_1| |\mathbf{p}_3| \cos \theta = \\
&= m_{D_s}^2 + m_{D_s^*}^2 - 2p_1^0 p_3^0 + 2|\mathbf{p}_1| |\mathbf{p}_3| \cos \theta,
\end{aligned} \quad (43)$$

and

$$\begin{aligned}
\text{Abs}(11b) &= \frac{-iG_F}{2\sqrt{2}} \int_{-1}^1 \frac{d^3\mathbf{P}_1}{2E_1(2\pi)^3} \frac{d^3\mathbf{P}_2}{2E_2(2\pi)^3} \times \\
&\times (2\pi)^4 \delta^4(p_B - p_1 - p_2) (-ig_{D_s K^* D^*}) \varepsilon_3 \cdot (p_1 + q) \times \\
&\times (-ig_{D_s^* K^* D}) \varepsilon_2 \cdot (-q) f_B f_{D_s} f_{D_s^*} \left[b_1 V_{cb} V_{cd}^* + \right. \\
&\left. + \left(2b_4 + \frac{1}{2} b_{4eW} \right) \right] \lambda_p \frac{F^2(q^2, m_{K^*}^2)}{T_2} = \\
&= \frac{-iG_F}{8\sqrt{2}\pi m_B} g_{D_s K^* D^*} g_{D_s^* K^* D} \int_{-1}^1 |P_1| d(\cos\theta) \times \\
&\times f_B f_{D_s} f_{D_s^*} \left[b_1 V_{cb} V_{cd}^* + \left(2b_4 + \frac{1}{2} b_{4eW} \right) \right] \times \\
&\times \lambda_p \frac{F^2(q^2, m_{K^*}^2)}{T_2} H_2, \tag{44}
\end{aligned}$$

where

$$\begin{aligned}
H_2 &= \varepsilon_{\mu\nu\alpha\beta} \varepsilon_{\rho\sigma\lambda\eta} \varepsilon_3^\mu \varepsilon_{K^*}^\nu p_1^\alpha p_3^\beta \varepsilon_2^\rho \varepsilon_{K^*}^\sigma p_2^\lambda p_4^\eta, \\
T_2 &= (p_1 - p_3)^2 - m_{K^*}^2 = p_1^2 + p_3^2 - \\
&- 2p_1^0 p_3^0 + 2\mathbf{p}_1 \cdot \mathbf{p}_3 - m_{K^*}^2, \tag{45} \\
q^2 &= m_1^2 + m_3^2 - 2E_1 E_3 + 2|\mathbf{p}_1||\mathbf{p}_3| \cos\theta = \\
&= m_{D_s}^2 + m_{D^*}^2 - 2p_1^0 p_3^0 + 2|\mathbf{p}_1||\mathbf{p}_3| \cos\theta.
\end{aligned}$$

The dispersion relation is

$$\text{Dis}11(m_B^2) = \frac{1}{\pi} \int_s^\infty \frac{\text{Abs}11a(s') + \text{Abs}11b(s')}{s' - m_B^2} ds'. \tag{46}$$

4.6. Final State Interaction

in $B^0 \rightarrow J/\psi\pi^0 \rightarrow D^{0*}\bar{D}^0$ Decay

The quark model diagram for $B^0 \rightarrow J/\psi\pi^0 \rightarrow D^{0*}\bar{D}^0$ decay is shown in Fig. 12, and the hadronic level diagrams are shown in Fig. 13. We have

$$\begin{aligned}
\text{Abs}(13a) &= \frac{-iG_F}{2\sqrt{2}} \int_{-1}^1 \frac{d^3\mathbf{P}_1}{2E_1(2\pi)^3} \frac{d^3\mathbf{P}_2}{2E_2(2\pi)^3} \times \\
&\times (2\pi)^4 \delta^4(p_B - p_1 - p_2) (-ig_{\pi DD^*}) \varepsilon_3 \cdot (p_1 + q) \times \\
&\times (-ig_{\psi DD}) \varepsilon_2 \cdot (-q) \left\{ 2m_\psi (\varepsilon_2 \cdot p_1) f_\pi A_0^{B\psi} \left[a_2 V_{cb} V_{cd}^* + \right. \right. \\
&\left. \left. + \left(a_3 + r_\chi^\psi (a_5 + a_7 + a_9) \right) \lambda_p \right] \right\} \frac{F^2(q^2, m_D^2)}{T_1},
\end{aligned}$$

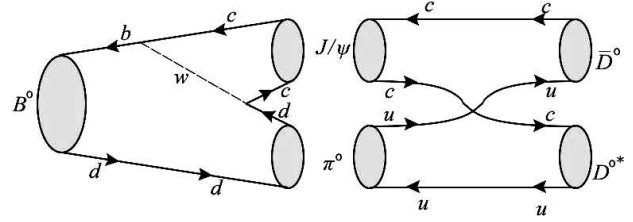


Fig. 12. Quark level diagram for $B^0 \rightarrow J/\psi\pi^0$

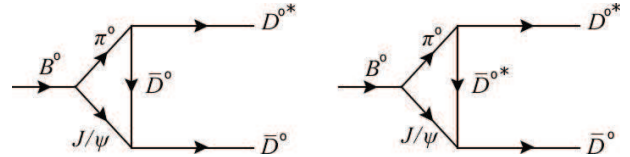


Fig. 13. HLL diagrams for the long-distance t -channel contribution to $B^0 \rightarrow D^{0*}\bar{D}^0$

$$\begin{aligned}
&= \frac{-iG_F}{8\sqrt{2}\pi m_B} g_{\pi DD^*} g_{\psi DD} \int_{-1}^1 |P_1| d(\cos\theta) \times \\
&\times \left\{ 2H_1 m_\psi f_\pi A_0^{B\psi} \left[a_2 V_{cb} V_{cd}^* + \left(a_3 + r_\chi^\psi \times \right. \right. \right. \\
&\left. \left. \left. \times (a_5 + a_7 + a_9) \right) \lambda_p \right] \right\} \frac{F^2(q^2, m_D^2)}{T_1}, \tag{47}
\end{aligned}$$

where

$$\begin{aligned}
H_1 &= (\varepsilon_2 \cdot p_1) (\varepsilon_2 \cdot p_4) (\varepsilon_3 \cdot p_1) = \\
&= \left(-p_1 \cdot p_4 + \frac{(p_1 \cdot p_2)(p_2 \cdot p_4)}{m_\psi^2} \right) \times \\
&\times \left(\frac{E_1 |p_3| - E_3 |p_1| \cos\theta}{m_B |p_3|} \right), \tag{48} \\
T_1 &= (p_1 - p_3)^2 - m_D^2 = p_1^2 + p_3^2 - \\
&- 2p_1^0 p_3^0 + 2\mathbf{p}_1 \cdot \mathbf{p}_3 - m_D^2, \\
q^2 &= m_1^2 + m_3^2 - 2E_1 E_3 + 2|\mathbf{p}_1||\mathbf{p}_3| \cos\theta = \\
&= m_\pi^2 + m_{D^*}^2 - 2p_1^0 p_3^0 + 2|\mathbf{p}_1||\mathbf{p}_3| \cos\theta,
\end{aligned}$$

and

$$\begin{aligned}
\text{Abs}(13b) &= \frac{-iG_F}{2\sqrt{2}} \int_{-1}^1 \frac{d^3\mathbf{P}_1}{2E_1(2\pi)^3} \frac{d^3\mathbf{P}_2}{2E_2(2\pi)^3} (2\pi)^4 \times \\
&\times \delta^4(p_B - p_1 - p_2) (-ig_{\pi DD^*}) \varepsilon_3 \cdot (p_1 + q) (-ig_{\psi DD}) \times \\
&\times \varepsilon_2 \cdot (-q) \left\{ 2m_\psi (\varepsilon_2 \cdot p_1) f_\pi A_0^{B\psi} \left[a_2 V_{cb} V_{cd}^* + \right. \right. \\
&\left. \left. + \left(a_3 + r_\chi^\psi (a_5 + a_7 + a_9) \right) \lambda_p \right] \right\} \frac{F^2(q^2, m_{D^*}^2)}{T_2},
\end{aligned}$$

$$\begin{aligned}
 &= \frac{-iG_F}{8\sqrt{2}\pi m_B} g_{\pi DD^*} g_{\psi DD} \int_{-1}^1 |P_1| d(\cos \theta) \times \\
 &\times \left\{ 2H_3 m_\psi f_\pi A_0^{B\psi} \left[a_2 V_{cb} V_{cd}^* + \right. \right. \\
 &\left. \left. + \left(a_3 + r_\chi^\psi (a_5 + a_7 + a_9) \right) \lambda_p \right] \right\} \frac{F^2(q^2, m_{D^*}^2)}{T_2}, \quad (49)
 \end{aligned}$$

where

$$\begin{aligned}
 H_3 &= m_3^2(p_1.p_2) - (p_1.p_3)(p_2.p_3) + \\
 &+ \left(\frac{E_2|p_3| - E_3|p_2|\cos\theta}{m_B|p_3|} \right) \times \\
 &\times [(p_B.p_1)(p_3.p_4) - (p_B.p_3)(p_1.p_4)], \\
 T_2 &= (p_1 - p_3)^2 - m_{D^*}^2 = p_1^2 + p_3^2 - \\
 &- 2p_1^0 p_3^0 + 2\mathbf{p}_1 \cdot \mathbf{p}_3 - m_{D^*}^2, \\
 q^2 &= m_1^2 + m_3^2 - 2E_1 E_3 + 2|\mathbf{p}_1||\mathbf{p}_3|\cos\theta = \\
 &= m_\pi^2 + m_{D^*}^2 - 2p_1^0 p_3^0 + 2|\mathbf{p}_1||\mathbf{p}_3|\cos\theta.
 \end{aligned} \quad (50)$$

The dispersion relation is

$$\text{Dis13}(m_B^2) = \frac{1}{\pi} \int_s^\infty \frac{\text{Abs13}a(s') + \text{Abs13}b(s')}{s' - m_B^2} ds'. \quad (51)$$

The decay amplitude via the HLL diagrams is

$$\begin{aligned}
 A(B^0 \rightarrow D^{0*} \bar{D}^0) &= \text{Abs}(3a) + \text{Abs}(3b) + \text{Abs}(5a) + \\
 &+ \text{Abs}(5b) + \text{Abs}(7a) + \text{Abs}(7b) + \text{Abs}(9a) + \text{Abs}(9b) + \\
 &+ \text{Abs}(11a) + \text{Abs}(11b) + \text{Abs}(13a) + \text{Abs}(13b) + \\
 &+ \text{Dis3}(m_B^2) + \text{Dis5}(m_B^2) + \text{Dis7}(m_B^2) + \\
 &+ \text{Dis9}(m_B^2) + \text{Dis11}(m_B^2) + \text{Dis13}(m_B^2). \quad (52)
 \end{aligned}$$

The branching ratio of $B^0 \rightarrow D^{0*} \bar{D}^0$ decay with $\eta = 0.8 \sim 1.6$ and experimental data (in units of 10^{-4})

η	0.8	1	1.2	1.4	1.6	EXP
BR	0.27 ± 0.04	0.62 ± 0.05	1.3 ± 0.07	2.2 ± 0.08	3.7 ± 0.10	<2.9

5. Numerical Results

The numerical values of effective coefficients a_i for the $\bar{b} \rightarrow \bar{d}$ transition at $N_c = 3$ are given by [11]

$$\begin{aligned}
 a_1 &= 1.05, \quad a_2 = 0.053, \\
 a_3 &= 0.0048, \quad a_4 = -0.046 - 0.012i, \\
 a_5 &= -0.0045, \quad a_6 = -0.059 - 0.012i, \\
 a_7 &= 0.00003 - 0.00018i, \quad a_8 = 0.0004 - 0.00006i, \\
 a_9 &= -0.009 - 0.00018i, \quad a_{10} = -0.0014 - 0.00006i.
 \end{aligned} \quad (53)$$

The relevant input parameters used are the following [12, 13, 14, 15]:

$$\begin{aligned}
 m_b &= 4.2 \pm 0.12 \text{ GeV}, \quad m_u = 1.7 \sim 3.1 \text{ MeV}, \\
 m_d &= 4.1 \sim 5.7 \text{ MeV}, \quad m_c = 1.29 \pm 0.08 \text{ GeV}, \\
 m_s &= 100 \pm 25 \text{ MeV}, \quad m_B = 5279 \pm 0.3 \text{ MeV}, \\
 m_D &= 187 \pm 0.2 \text{ MeV}, \quad m_{D^*} = 2010.2 \pm 0.17, \\
 m_K &= 493.6 \pm 0.016 \text{ MeV}, \quad m_{K^*} = 891 \pm 0.26 \text{ MeV}, \\
 m_{D_s} &= 1968.4 \pm 0.34 \text{ MeV}, \quad m_{D_s^*} = 2010.2 \pm 0.17, \\
 m_\pi &= 139.5 \text{ MeV}, \quad m_\rho = 775.4 \pm 0.34 \text{ MeV}, \\
 m_{J/\psi} &= 3.096 \text{ GeV}, \quad f_B = 176 \pm 42 \text{ MeV}, \\
 f_\pi &= 130.7 \pm 0.46 \text{ MeV}, \quad f_\rho = 211 \text{ MeV}, \\
 f_K &= 159.8 \pm 1.84 \text{ MeV}, \quad f_{K^*} = 217 \pm 5 \text{ MeV}, \\
 f_D &= 222.6 \pm 19.5 \text{ MeV}, \quad f_{D^*} = 230 \pm 20 \text{ MeV}, \\
 f_{D_s} &= 294 \pm 27 \text{ MeV}, \quad f_{D_s^*} = 266 \pm 32 \text{ MeV}, \\
 V_{ub} &= 0.0043 \pm 0.0003, \quad V_{ud} = 0.97 \pm 0.0002, \\
 V_{cb} &= 0.0416 \pm 0.0006, \quad V_{cd} = 0.230 \pm 0.011, \\
 A_0^{BD^*}(m_{D^*}^2) &= 2.5, \quad A_0^{BK^*}(m_{K^*}^2) = 0.45, \\
 A_0^{BD^*}(m_{D^*}^2) &= 2.5, \quad A_0^{BK^*}(m_{K^*}^2) = 0.45, \\
 A_0^{B\rho}(m_\rho^2) &= 0.3, \quad A_0^{BD_s^*}(m_{D_s^*}^2) = 0.3, \\
 \phi &= -55(PP), \quad \phi = -70(VP), \\
 \phi &= -20(PV), \quad \phi = 0.5, \\
 \Lambda_{QCD} &= 0.225, \quad G_F = 1.166 \times 10^{-5}, \\
 g_{DKD_s^*} &= 18.34, \quad g_{D^*K^*D_s} = 2.79, \\
 g_{D^*KD_s} &= 18.37, \quad g_{K^*D_sD} = 2.59, \\
 g_{D\rho D^*} &= 2.82, \quad g_{\rho\rho D} = 3, \\
 g_{\psi DD} &= 7.7, \quad g_{D^*K^*D} = 3, \quad g_{\psi D^*D} = 8.64. \quad (54)
 \end{aligned}$$

By using the input parameters, we have obtained the value of branching ratio for $B^0 \rightarrow D^{0*} \bar{D}^0$ decay within the QCDF method to be

$$BR(B^0 \rightarrow D^{0*} \bar{D}^0) = (0.13 \pm 0.11) \times 10^{-4}. \quad (55)$$

We note that our estimate of the branching ratio of the $B^0 \rightarrow D^{0*} \bar{D}^0$ decay according to the QCDF method seems less than the experimental result. Before calculating the $B^0 \rightarrow D^{0*} \bar{D}^0$ decay amplitude via FSI, we have to compute the intermediate state amplitude. We are able to calculate the branching ratio of the $B^0 \rightarrow D^{0*} \bar{D}^0$ decay with different values of η , which are shown in the table.

6. Conclusion

We have calculated the contribution of the t -channel FSI, that is, of inelastic re-scattering processes to the branching ratio of the $B^0 \rightarrow D^{0*} \bar{D}^0$ decay. For evaluating the FSI effects, we have only considered the absorptive part of the HLL, because both hadrons, which are produced via the weak interaction, are on their mass shells. We have calculated the branching ratio of the $B^0 \rightarrow D^{0*} \bar{D}^0$ decay by using the QCDF and FSI methods. The experimental value of this decay is less than 2.9×10^{-4} . According to the QCDF and FSI methods, our results are $BR(B^0 \rightarrow D^{0*} \bar{D}^0) = (0.13 \pm 0.11) \times 10^{-4}$ and $(2.2 \pm 0.08) \times 10^{-4}$, respectively. We have introduced the phenomenological parameter η , which can be determined from the measured rates with the expected value of the order of 1, in the form factor. For a given exchanged particle, we have used $\eta = 0.8 \sim 1.6$. If $\eta = 1.4$ is selected, the branching ratio of the $B^0 \rightarrow D^{0*} \bar{D}^0$ decay approaches the experimental value bound.

1. X. Liu, X.Q. Zeng, and X.Q. Li, Phys. Rev. D **74**, 34610 (2006).
2. B. Borasoy and E. Marco, Phys. Rev. D **67**, 114016(2003).
3. X. Liu, Z.T. Wei, and X.Q. Li, The European Physical Journal C **59**, 683 (2009).
4. C.H. Chen, Phys. Rev. A **67**, No. 6 (2003).
5. Y.S. Oh, T. Song, and S.H. Lee, Phys. Rev. C **63**, No. 3 (2001).
6. H.Y. Cheng, C.K. Chua, and A. Soni, Phys. Rev. D **71**, No. 1 (2005).
7. Particle Data Group, Phys. Rev. D **86**, 010001 (2012).
8. M. Beneke, G. Buchalla, M. Neubert, and C.T. Sachrajda, Nucl. Phys. B **606**, 245 (2001).
9. B. Zhang, X. Lu, and S.L. Zhu, Chinese Phys. Lett. **24**, No. 9 (2007).
10. C.D. Lu, Phys. Rev. D **73**, No. 3 (2006).
11. A. Ali, G. Kramer, and C.D. Lu, Phys. Rev. D **58**, No. 9 (1998).
12. H.Y. Cheng, C.K. Chua, and A. Soni, Phys. Rev. D **71**, 014030 (2005).
13. C.D. Lu, Y.L. Shen, and W. Wang, Phys. Rev. D **73**, 034005 (2006).
14. B. Mohammadi and H. Mehraban, Int. J. of Mod. Phys. A **27**, No. 11 (2012).
15. K. Azizi, R. Khosravi, and F. Falahati, Int. J. of Mod. Phys. A **24**, No. 31 (2009).

Received 05.04.14

X. Мехрабан, А. Асаді

ЕФЕКТИ ВЗАЄМОДІЇ

В КІНЦЕВОМУ СТАНІ В РОЗПАДІ $B^0 \rightarrow D^{0*} \bar{D}^0$

Резюме

Розрахований ексклюзивний розпад $B^0 \rightarrow D^{0*} \bar{D}^0$ методом КХД факторизації і методом, що враховує взаємодію в кінцевому стані. Розрахунок по першому методу дав занижені результати порівняно з експериментом, що свідчило про необхідність врахування взаємодії в кінцевому стані. В даному розпаді $D^+ D^{*-}$, $K^+ K^-$, $\rho^+ \pi^-$, $\rho^0 \pi^0$, $D_s^- D_s^+$ і $J/\psi \pi^0$ з обміном $\pi^- (\rho^-)$, $D_s^- (D_s^{*-})$, $D^- (D^{*-})$, $\bar{D}^0 (\bar{D}^{0*})$ і $K^- (K^{*-})$ мезонами вибрані як проміжні стани і розраховувалися за першим методом. У другому методі результати розрахунків залежать від феноменологічного параметра η . Інтервал зміни цього параметра вибрано від 0,8 до 1,6. Знайдено, що для $\eta = 1,4$ величина коефіцієнта розгалуження узгоджується з експериментальним значенням для $B^0 \rightarrow D^{0*} \bar{D}^0$ розпаду: менше $2,9 \cdot 10^{-4}$. Наші розрахунки по першому і другому методах дали, відповідно, $(0,13 \pm 0,11) \cdot 10^{-4}$ і $(2,2 \pm 0,08) \cdot 10^{-4}$.